

Pb isotope geochemistry and reappraisal of Sr-Nd isotopes of the Cerro Morado basic magmatism (Ischigualasto-Villa Union Triassic basin, NW Argentina): Implications for the mantle sources

Carlos Augusto Sommer^{1*}, Carla Joana S. Barreto², Jean Michel Lafon³, Evandro Fernandes de Lima¹, Felipe Marcelo Alexandre¹, Farid Chemale Jr.⁴, Edinei Koester¹

ABSTRACT: Sr-Nd-Pb isotopic signatures were determined for silica-undersaturated hypabyssal alkaline basic rocks of the Los Baldecitos Formation in the Cerro Morado area, situated in the Ischigualasto — Vale de la Luna Provincial Park (northernmost San Juan Province, Argentina). The basic rocks show slight variations of the Sr-Nd-Pb isotopes and similar behavior of whole-rock geochemistry, which suggest a single source for the Cerro Morado volcanic rocks. The present-day Pb isotopic data show moderately radiogenic Pb compositions ($^{206}\text{Pb}/^{204}\text{Pb} = 18.31 - 18.35$), in addition to low values of $^{87}\text{Sr}/^{86}\text{Sr}$ initial ratios of $0.70314 - 0.70386$ and highly radiogenic Nd initial isotopic compositions ($+7.1 < \epsilon_{\text{Nd}}(228\text{Ma}) < +9.3$), which point to a PREMA mantle reservoir signature for the alkaline basalts with little evidence of crustal contamination. The involvement of a HIMU component in the source, previously suggested for the Cerro Morado volcanics, should be disregarded in the light of the Pb isotopic signature. The Sr-Nd signature together with Nd- T_{DM} model ages not older than 295 Ma does not support the involvement of an ancient crust.

KEYWORDS: Ischigualasto-Villa Unión Triassic Basin; Silica Undersaturated Rocks; Northwestern Argentina; Sr-Nd-Pb Isotopes.

INTRODUCTION

The Ischigualasto-Villa Union Basin, northwestern Argentina, is part of a system of continental basins generated mainly by extensional tectonics related to the breakup of the Gondwana supercontinent. This basin corresponds to a hemigabren elongated in a NW-SE direction (Milana & Alcober 1994) and is filled by clastic continental sedimentation — mainly fluvial-lacustrine — and volcanic and hypabyssal rocks of basic to intermediary composition. This volcanism is traditionally related to structures resulting from reactivation of Paleozoic lineaments during the Neotriassic. One of the main

occurrences of silica-undersaturated alkaline basic hypabyssal rocks (Los Baldecitos Formation) is observed as a sill in the Cerro Morado area, overlying a basal unit formed by sedimentary rocks (Mesotriassic Chanãres Formation). Fieldwork, petrography and whole-rock geochemistry show that this magmatism was established in an intraplate environment in which mantle sources were responsible for the emplacement of the sill on the top of the Chanãres Formation (Alexandre *et al.* 2009).

The aim of this paper was to discuss mantle sources of the basic rocks of Cerro Morado and to better understand the role of Triassic magmatism in the Villa Union Basin, based on a reappraisal of previously published geochemical and

¹Instituto de Geociências, Universidade Federal do Rio Grande do Sul – Porto Alegre (RS), Brazil. E-mails: casommer@sinos.net, evandro.lima@ufrgs.br, koester@ufrgs.br, fmalexandre@pop.com.br

²Centro de Tecnologia e Geociências, Universidade Federal de Pernambuco – Recife, (PE), Brazil. E-mail: carlabarreto.geo@hotmail.com

³Instituto de Geociências, Universidade Federal do Pará – Belém (PA), Brazil. E-mail: lafonjm@ufpa.br

⁴Universidade do Vale do Rio dos Sinos – São Leopoldo (RS), Brazil. E-mail: faridchemale@gmail.com

*Corresponding author.

Manuscript ID: 20170106. Received in: 09/08/2017. Approved in: 12/10/2017.

Sr-Nd isotope data, together with new Pb isotope data on the same rocks. A specific purpose was to test the hypothesis of a previously suggested HIMU mantle component as a source of these basic rocks (Alexandre *et al.* 2009).

GEOLOGICAL SETTING

The basement of the Ischigualasto–Villa Union Basin is composed of igneous and metamorphic rocks from the Precambrian Igneous Metamorphic Valle Fertil Complex (Bossi 1971) and Eopermian sedimentary rocks from the Patquia Formation of the Paganzo Group. The basin is bounded by Valle Fertil lineament to the west and the Sierra de los Tarjados to the east (Stipanovic & Bonaparte 1979) (Fig. 1).

The basal units of the basin are composed by clastic continental sequences of the Talampaya and Tarjados formations of lower Triassic age. The overlying Chañares Formation is composed of volcanogenic conglomerates with volcanic clasts immersed in a tuffaceous groundmass. These conglomerates, together with sandstones and mudstones, characterize a sequence of rocks related to debris flow (Milana & Alcober 1994). Intrusive in this unit, occur the the hypabyssal rocks of Cerro Morado, which correspond to Los Baldecitos Formation. This volcanic sequence includes olivine-bearing diabbases in the base, and porphyritic tephrites that predominate at the top (Alexandre *et al.* 2009). The Los Baldecitos Formation is stratigraphically succeeded by the Los Colorados Formation, which consists of reddish sandstone with tabular geometry and parallel stratification. Channeled conglomeratic bodies are observed in the central portions, often interleaved with Fe oxide-rich thin beds in the upper part of the formation (Kokogian *et al.* 1987, Lopez Gamundi *et al.* 1989, Limarino *et al.* 1990).

The magmatism of the Los Baldecitos Formation have basic to intermediate composition and occurs as lavas, sills, and associated laccolith. These sills and laccoliths are intrusive within Chañares deposits. Ar-Ar dating indicates an age of 228 ± 2 Ma (Chemale Jr. personal communication) and previous whole-rock geochemistry and Nd-Sr isotope led Alexandre *et al.* (2009) to consider this magmatism as typical intraplate alkaline basalts affected by metasomatism, whose source may be related to a HIMU reservoir.

GEOLOGY AND PETROGRAPHY OF THE CERRO MORADO ROCKS

The basic hypabyssal rocks of Los Baldecitos Formation show tabular subhorizontal geometry, which is conformable with the deposits of the Chañares Formation (Fig. 2A).

The basic rocks occur as a sill nearly 200 m thick and 1,200 m length (N-S), showing a massive aspect in the entire body, with sparse vesicles. Ophitic, subophitic and poikilitic textures are predominant in these intrusive bodies. Additionally, an irregular jointing with a columnar pattern, perpendicular to the walls of the sill, is common.

The basal part of the sill is approximately 30 m thick and consists of a porphyritic olivine-bearing diabase, where plagioclase phenocrysts and subordinate olivine are predominant (Figs. 2B and 2C). These phenocrysts are encompassed by a matrix composed of plagioclase, clinopyroxene, opaque minerals and apatite (Fig. 2D), and predominant subophitic, intergranular, ophitic, and branching textures (Fig. 2D). In the intermediate and upper portions of the sill, tephrites predominate with porphyritic and glomeroporphyritic textures and show a diffuse contact with the olivine-bearing diabase. The tephrites exhibit imbrication of plagioclase crystals, suggesting cumulate processes occurring locally (Fig. 2E), as well as trachytic and branching textures. The matrix is finely to medium grained, composed by plagioclase, nepheline, analcime, clinopyroxene, opaque minerals, and apatite (Figs. 2F and 2G). In the intermediate portion, subvertical fractures are filled by hydraulic breccias, consisted of moderately altered tephrite fragments surrounded by a matrix of banded chalcedony, carbonate, and bipyramidal quartz. Micro-vesicles are restricted to some samples, generally filled by quartz, chlorite, smectite and carbonate (Fig. 2H).

ANALYTICAL PROCEDURES FOR WHOLE-ROCK GEOCHEMISTRY AND Sm-Nd, Rb-Sr AND Pb-Pb ISOTOPE

The whole-rock chemical analysis were performed at ACME Laboratories Ltd (Canada) in which the 4A+4B package was used to analyze major oxides by Inductively Coupled Plasma Atomic Emission Spectrometry (ICP-AES). Trace elements and rare earth elements (REE) were analyzed by Inductively Coupled Plasma Atomic Mass Spectrometry (ICP-MS).

Sr, Nd, Pb isotope analyses were carried out at the Isotope Geology Laboratory of the *Universidade Federal do Rio Grande do Sul* with a VG Sector 54 multicollector thermal ionization mass spectrometer. For the sample digestion procedure, rock samples were powdered in agate mortar at a grain size lower than 200 mesh, where, ~100 mg of the rock sample were mixed with a $^{149}\text{Sm}/^{150}\text{Nd}$ and $^{87}\text{Rb}/^{84}\text{Sr}$ spike and dissolved with HF-HNO₃ and HCl in 7 mL Teflon vials on a hot plate for seven days. Rb, Sr and REE were

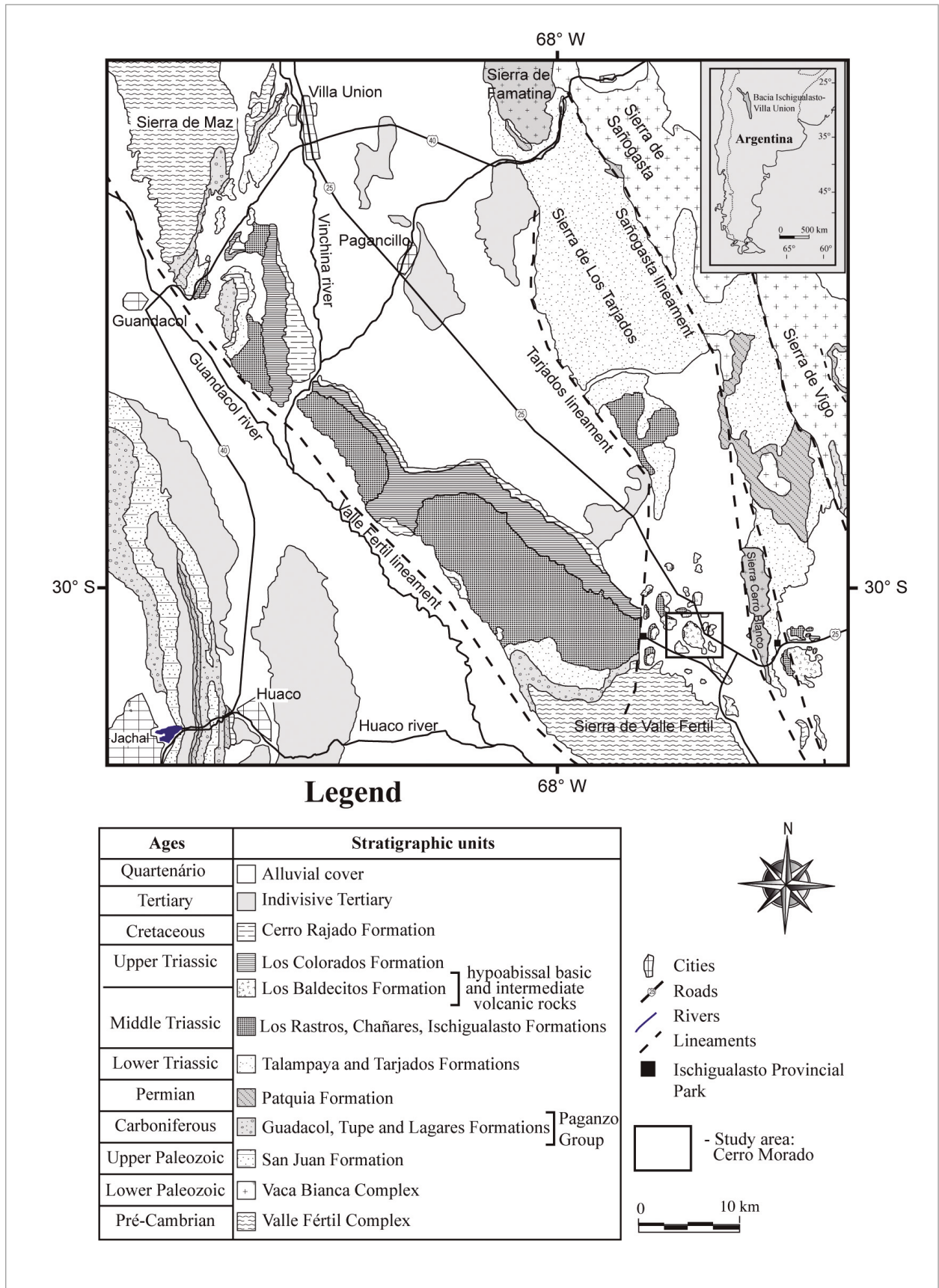


Figure 1. Geologic map of the Ischigualasto-Villa Union Basin. Modified from Caselli (2000).

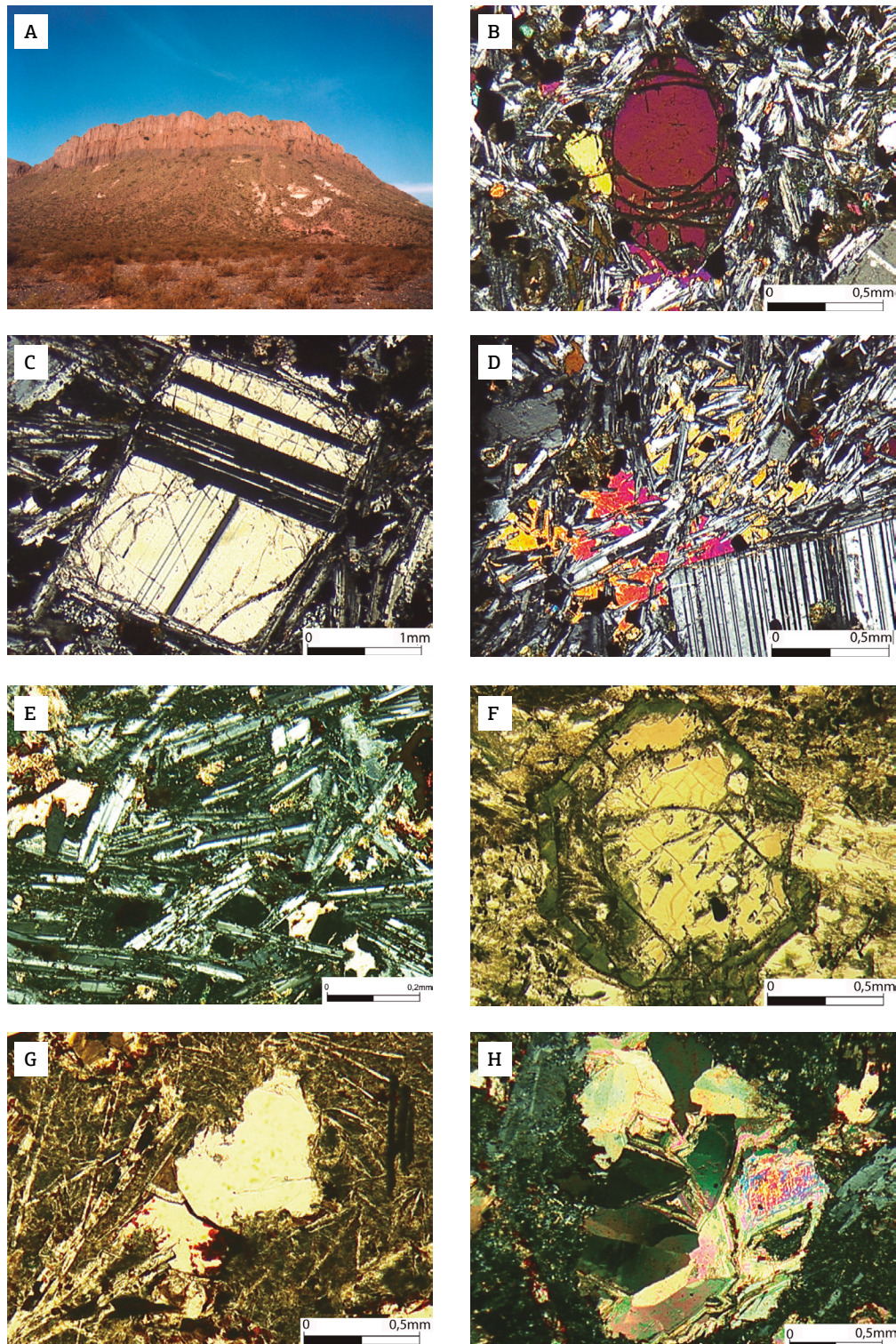


Figure 2. Field and microscopic features of the Cerro Morado (cf. Alexandre *et al.* 2009). (A) Front view of the Cerro Morado, including the contact relationship between the two units; (B) olivine euhedral phenocryst embedded in fine-grained matrix of the diabase; (C) plagioclase phenocryst of the diabase; (D) subophitic texture in diabase; (E) imbricated plagioclase crystals in the matrix of the tephrite; (F) augite phenocryst with rims altered to chlorite and iron; (G) analcite phenocryst with anhedral habit immersed in matrix with branching texture; (H) vesicle filled by carbonate.

purified by using cation exchange chromatography with a DOWEX AG 50X8 resin (200–400 mesh). Nd and Sm were separated from the other REE by using exchange columns with Di-(2-ethylhexyl) orthophosphoric acid (HDEHP) resin (50–100 nm). Pb was purified using anion exchange DOWEX AG-1X8 resin (200–400 mesh).

For the isotopic analyses, Rb, Sr, Sm and Pb were run on Re single filaments and Nd on Ta-Re triple filaments. The Pb concentrates were deposited with silica gel. The Sr and Nd isotopic compositions were normalized to $^{86}\text{Sr}/^{88}\text{Sr} = 0.1194$ and $^{146}\text{Nd}/^{144}\text{Nd} = 0.7219$, respectively. Pb was corrected from mass discrimination by using a factor of $0.1\% \text{ amu}^{-1}$ based on 38 analyses of NBS-981 reference material. Repeated analyses of NBS 987 and La Jolla reference material furnished $^{87}\text{Sr}/^{86}\text{Sr}$ and $^{143}\text{Nd}/^{144}\text{Nd}$ values of 0.71026 ± 0.000011 (1σ ; $n = 100$) and 0.511848 ± 0.000021 (1σ ; $n = 100$), respectively. The blanks used for the procedure were lower than 500 pg for Rb and Sm, and than 60 pg, 150 pg and 100 pg for Sr, Nd and Pb, respectively. Typical analytical errors for $^{87}\text{Rb}/^{86}\text{Sr}$, $^{147}\text{Sm}/^{144}\text{Nd}$ and $^{208,207,206}\text{Pb}/^{204}\text{Pb}$ ratios did not exceed 0.1%. Nd-T_{DM} model ages were calculated according to the Depleted Mantle model of De Paolo (1981). The decay constants were those recommended by Steiger and Jäger (1977) for ^{87}Rb and by Lugmair and Marti (1978) for ^{147}Sm .

WHOLE-ROCK GEOCHEMISTRY

The high values of Loss on Ignition (LOI) obtained in the tephrite samples (Tab. 1) due to carbonation of feldspathoids, and high values in the olivine-bearing diabase sample do not allow the classification of the rocks in the Total-Alkali ($\text{Na}_2\text{O} + \text{K}_2\text{O}$) versus silica (SiO_2) (TAS) diagram, as recommended by International Union of Geological Sciences (IUGS). We used the Nb versus $\text{Zr}/\text{TiO}_2 * 0.0001$ diagram (Winchester & Floyd 1977), which establishes the relationship between major and trace elements with low degree of mobility. In this diagram, the Cerro Morado rocks occupy the alkali basalts field (Fig. 3). The behavior of major and trace elements, when correlated to the differentiation index ($\text{DI} = \text{Ab} + \text{Or} + \text{Q} + \text{Ne}$, normative — Thornton and Tuttle 1960), suggests a differentiation process by mineral fractionation (Figs. 4 and 5). The samples show inverse correlations of Al_2O_3 , CaO and Sr and positive correlation of K_2O with DI, which suggest a major participation of plagioclase toward the olivine-bearing diabase. The dispersion of Fe_2O_3 ($\text{FeO} + \text{Fe}_2\text{O}_3$) and TiO_2 contents may reflect fractionation and accumulation of mafic phases. The MgO, Ni, Cr and Co contents are very low. Ba, Nb, Y and Zr show an incompatible behavior in relation to DI. The Rb contents

also display a positive correlation with DI, which is coherent with K_2O contents (Fig. 5).

When normalized to oceanic island basalts (OIB) (Sun & McDonough 1989), the samples show higher values of Rb, Ba and K in relation to U and Th (Fig. 6A), which suggests some remobilization of low ionic potential elements by aqueous fluids.

The REE, when normalized to chondrites (Nakamura 1974), show a weak enrichment of Light Rare Earth Elements (LREE) in relation to Heavy Rare Earth Elements (HREE) ($\text{La}/\text{Yb} = 9.4\text{--}11.1$) (Fig. 6B). This signature is common in within-plate alkaline basalts (Cullers & Graf 1984, Wilson 1989). The small variation of Eu/Sm ratio ($0.313\text{--}0.387$) can be attributed to variations in the plagioclase contents, suggesting glomeroporphyritic accumulations.

In the $\text{Zr}/4\text{-Y-Nb} * 2$ diagram (Meschede 1986), the samples occupy the within-plate alkaline basalts field (Fig. 7A). Similar behavior is observed in the $\text{Th-Hf}/3\text{-Nb}/16$ (Wood 1980) and $\text{Zr-Zr}/\text{Y}$ diagrams (Pearce & Cann 1973) (Figs. 7B and 7C). In the Th/Yb versus Ta/Yb diagram (Pearce 1983), the alkali basalts plot close to the OIB field (Fig. 7D), which reinforces the geochemical signature defined by incompatible element pattern.

Sr-Nd-Pb ISOTOPE GEOCHEMISTRY

The Sr, Nd, and Pb isotope analyses obtained in one sample of olivine-bearing diabase and seven from tephrites are shown in Tab. 2 and Figs. 8, 9, 10 and 11. The initial $^{87}\text{Sr}/^{86}\text{Sr}$ and $^{143}\text{Nd}/^{144}\text{Nd}$ ratios were re-calculated to an age of 228 Ma. As Pb concentrations were not analyzed in the whole-rock geochemistry analyses, the corrections of the initial Pb ratios were not possible, thus using present-day Pb isotope compositions. The Cerro Morado rocks show initial $^{87}\text{Sr}/^{86}\text{Sr}$ ratios ranging from 0.70314 to 0.70386, and $\epsilon_{\text{Nd}(228 \text{ Ma})}$ values ranging from +7.1 to +9.3 with Nd-T_{DM} ages between 93 and 295 Ma. Present-day Pb isotope compositions range from 18.319 to 18.357 for $^{206}\text{Pb}/^{204}\text{Pb}$; 15.509 to 15.518 for $^{207}\text{Pb}/^{204}\text{Pb}$; and 37.834 to 37.880 for $^{208}\text{Pb}/^{204}\text{Pb}$.

In the $^{143}\text{Nd}/^{144}\text{Nd}_i$ versus $^{87}\text{Sr}/^{86}\text{Sr}_i$ diagram (Fig. 8), the samples exhibit high $^{143}\text{Nd}/^{144}\text{Nd}_i$ and low $^{87}\text{Sr}/^{86}\text{Sr}_i$ ratios, within the mantle array, close to the PREMA reservoir. In the Pb isotopic diagrams (Fig. 9), the samples plot below of the Northern Hemisphere Reference Line (NHRL) reference line and lying close to the PREvalent (PREMA) mantle reservoir field, similarly to the Nd-Sr isotopic signature.

In both $^{206}\text{Pb}/^{204}\text{Pb}$ versus $^{87}\text{Sr}/^{86}\text{Sr}$ and $^{206}\text{Pb}/^{204}\text{Pb}$ versus $^{143}\text{Nd}/^{144}\text{Nd}$ diagrams (Fig. 10), the studied rocks show a similar behavior and plot together overlapping the PREMA mantle reservoir field, besides plotting away from the HIMU field.

Sr-Nd-Pb isotope geochemistry of the Cerro Morado basic
magmatism (NW Argentina): Implications for the mantle sources

Table 1. Major and trace element geochemical data of the Cerro Morado rocks.

Rock type	Tephrite	Olivine-bearing diabase						
Sample	TM 4A	TM 6B	TM 7A	TM8 B	TM9 A	TM 10	TM 11	TM 12 A
<i>Major elements (wt.%)</i>								
SiO ₂	47.88	48.40	49.29	47.6	48.25	46.74	49.35	48.97
TiO ₂	2.51	2.33	2.16	2.14	2.31	2.15	1.68	2.15
Al ₂ O ₅	13.91	16.46	14.3	17.04	15.75	17.25	19.66	17.36
Fe ₂ O ₃	10.88	8.77	11.20	10.01	10.87	9.35	7.07	11.13
MnO	0.18	0.17	0.16	0.16	0.19	0.20	0.13	0.17
MgO	1.72	1.34	1.58	1.23	1.55	1	0.75	2.62
CaO	6.84	7.83	5.26	7.24	6.20	8.11	8.84	7.05
Na ₂ O	4.26	3.96	4.34	4.31	4.12	4.48	4.48	4.52
K ₂ O	2.63	1.92	3.28	1.86	2.42	2.32	1.70	1.95
P ₂ O ₅	0.9	0.96	0.72	0.86	0.95	0.86	0.63	0.78
LOI	7.21	6.58	6.61	6.19	6.49	6.46	4.8	2.59
Total	98.92	98.72	98.90	98.64	99.10	98.92	100.13	99.29
<i>Trace elements (ppm)</i>								
Rb	26.5	28.1	33.4	25.9	33.1	24.5	18.4	18.6
Ba	635	533	859	542	597	543	368	480
Sr	460	670	418	684	578	713	932	772
Nb	46.4	36.2	52.9	34	45.2	34.7	26	35.2
Zr	378.3	278.3	440.7	254.9	359.4	288	204.8	279
Y	44.1	35.3	44.4	31.3	41.2	35.2	23.5	31.5
Ni	-	-	-	-	-	28.7	20.8	-
Co	16.2	17	14.6	16	16.7	12.5	12.5	21.3
Hf	8.6	6.4	9.8	5.7	7.8	6.5	4.6	6.1
Ta	3	2.3	3.3	2	2.7	2.4	1.6	2.1
Th	3.7	2.5	4	2.2	3.2	2.7	1.9	2.6
U	1.2	0.8	1.4	0.8	1	0.9	0.7	0.9
La	40.1	34.7	41.9	29.3	38.4	31.8	23.8	31.1
Ce	88.6	76.3	90	64.9	83.3	69.1	52.2	68.1
Nd	46	39.6	45.6	35.3	44.4	36.2	27.9	35.8
Sm	10.9	9.4	10.4	8.1	10	8.3	6.1	8.1
Eu	3.4	3.2	3.3	2.9	3.4	3	2.4	2.8
Gd	10.5	8.9	9.9	7.6	9.6	8	5.9	7.6
Dy	9.2	7.2	9	6.5	8.3	6.8	4.9	6.5
Ho	1.8	1.3	1.7	1.2	1.5	1.3	0.9	1.2
Er	5	3.7	4.9	3.3	4.4	3.6	2.5	3.3
Yb	4.2	3.1	4.5	2.9	3.8	3.2	2.2	2.9
Lu	0.6	0.4	0.6	0.4	0.5	0.4	0.3	0.4

All Fe expressed as Fe₂O₃

DISCUSSION AND CONCLUSIONS

The diabase and tephrite samples of Cerro Morado show slight variations of their Sr-Nd-Pb isotopic composition, although all of the samples occupy the same field in the isotopic diagrams (Figs. 8, 9, 10 and 11). This suggests a same source for all volcanic rocks. The similar whole-rock geochemical behavior of all studied rocks reinforces this assumption.

The Sr-Nd isotopic data previously obtained for the Cerro Morado rocks suggested that their source was related to HIMU type mantle reservoir (Alexandre *et al.* 2009). However, in this previous study, the mantle reservoir fields were not recalculated to crystallization age, which would shift their positions. Additionally, in the geochemical comparison by Chart 1 from Alexandre *et al.* (2009), the samples move away from HIMU basalt compositions. The new set of Pb isotopic data obtained in this paper definitively discard the HIMU reservoir as a possible source for the

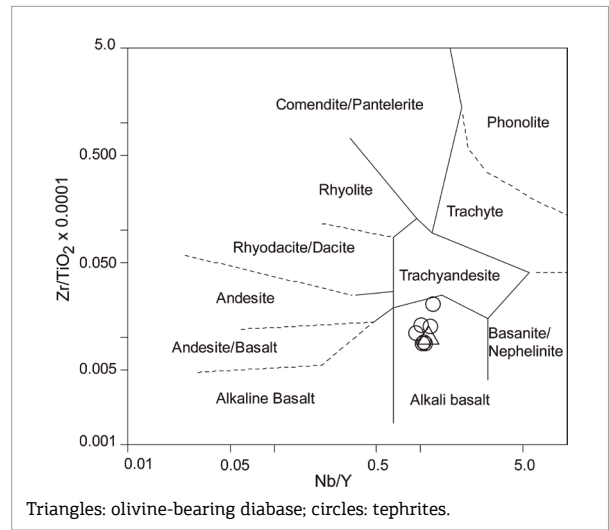


Figure 3. Geochemical diagram of characterization of the Cerro Morado rocks (cf. Alexandre *et al.* 2009). Nb/Y vs Zr/TiO₂*0.0001 diagram (Winchester & Floyd 1977) where the samples occupy the alkali basalt field.

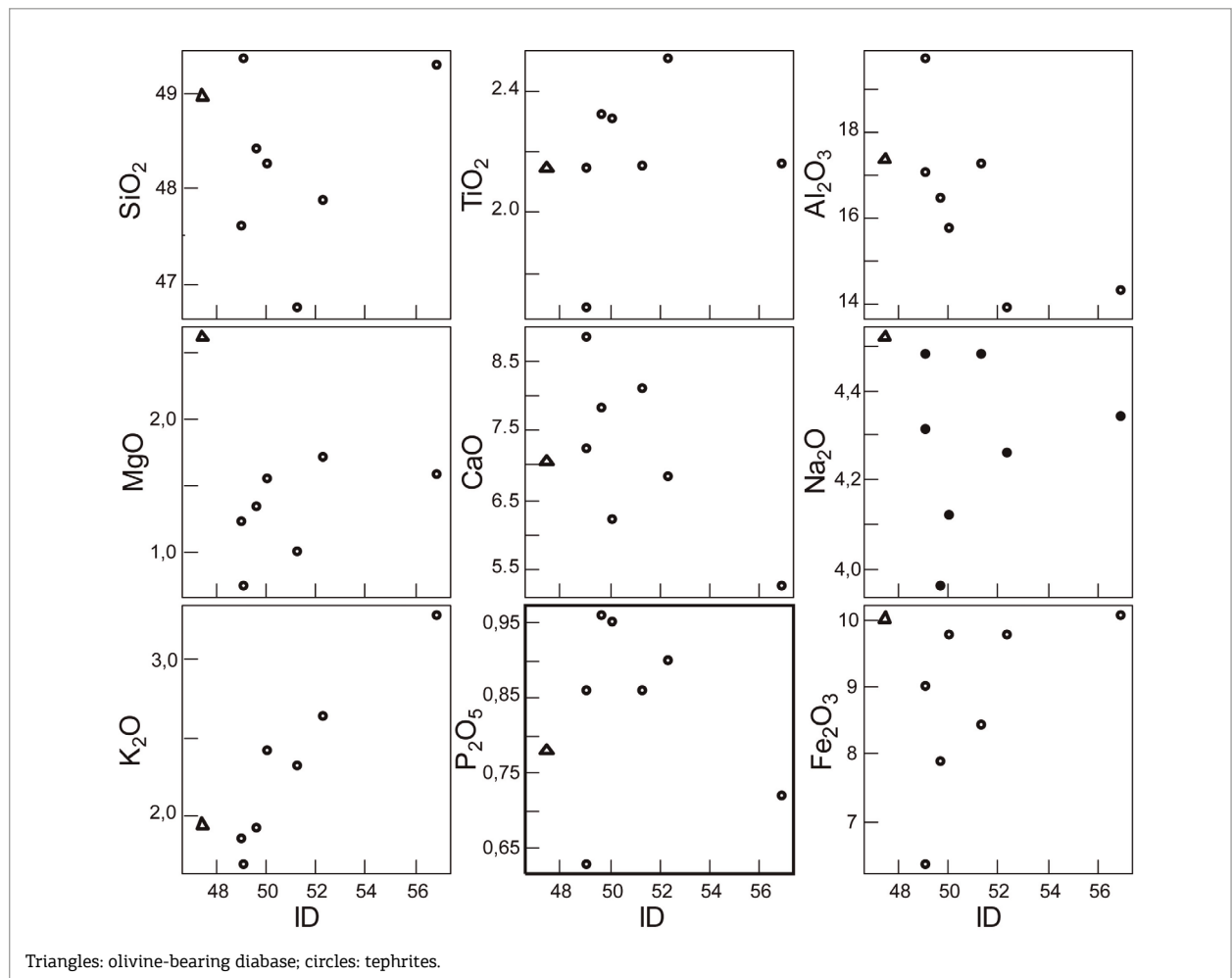


Figure 4. Major and minor element variation diagrams versus differentiation index (DI) for the Cerro Morado rocks (cf. Alexandre *et al.* 2009).

Cerro Morado rocks (Figs. 9 and 10). According to the moderately radiogenic Pb compositions ($^{206}\text{Pb}/^{204}\text{Pb} = 18.31\text{--}18.35$), in addition to low values of $^{87}\text{Sr}/^{86}\text{Sr}$ initial

ratios of $0.70314\text{--}0.70386$ and radiogenic Nd compositions ($\epsilon_{\text{Nd}}(228\text{ Ma}) = +7.1\text{ to }+9.3$), we argue that the Cerro Morado rocks show Prevalent mantle reservoir signature

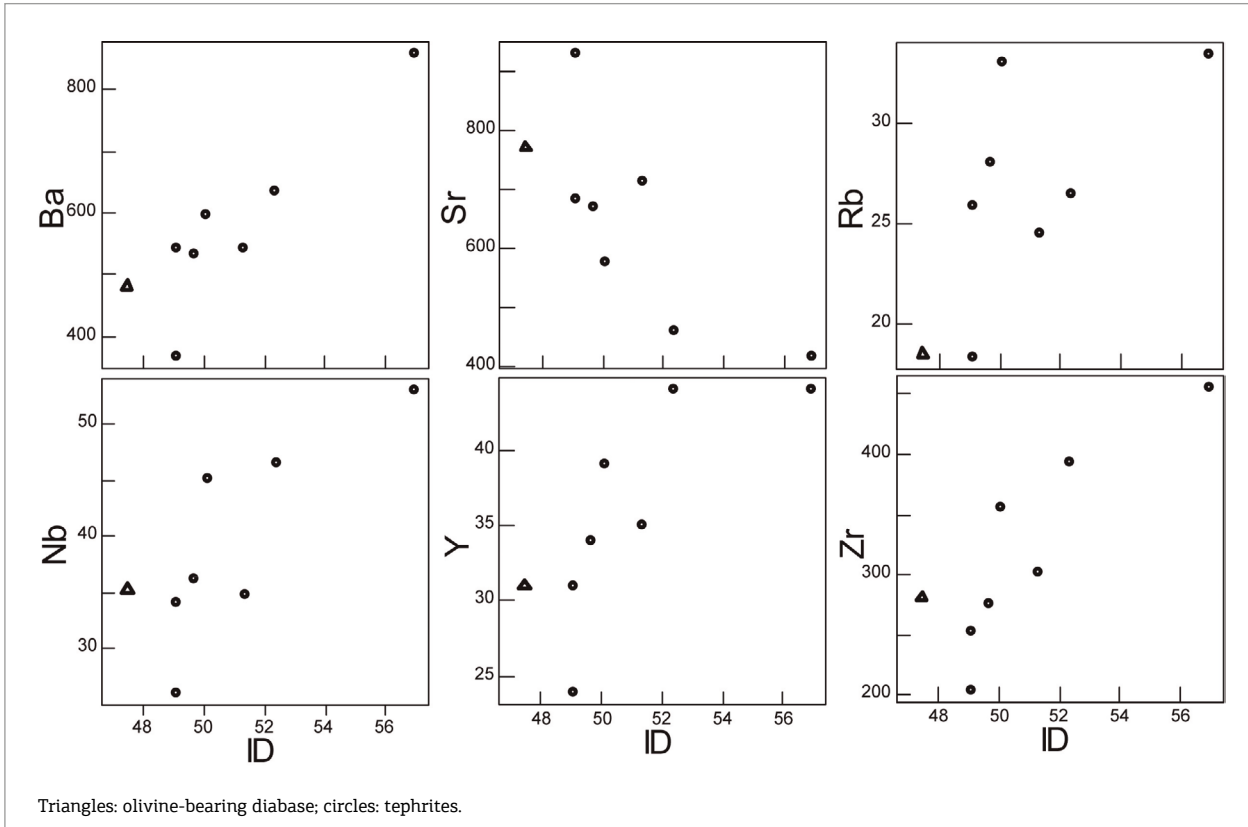


Figure 5. Trace element variation diagrams versus differentiation index (DI) for the Cerro Morado rocks (cf. Alexandre *et al.* 2009).

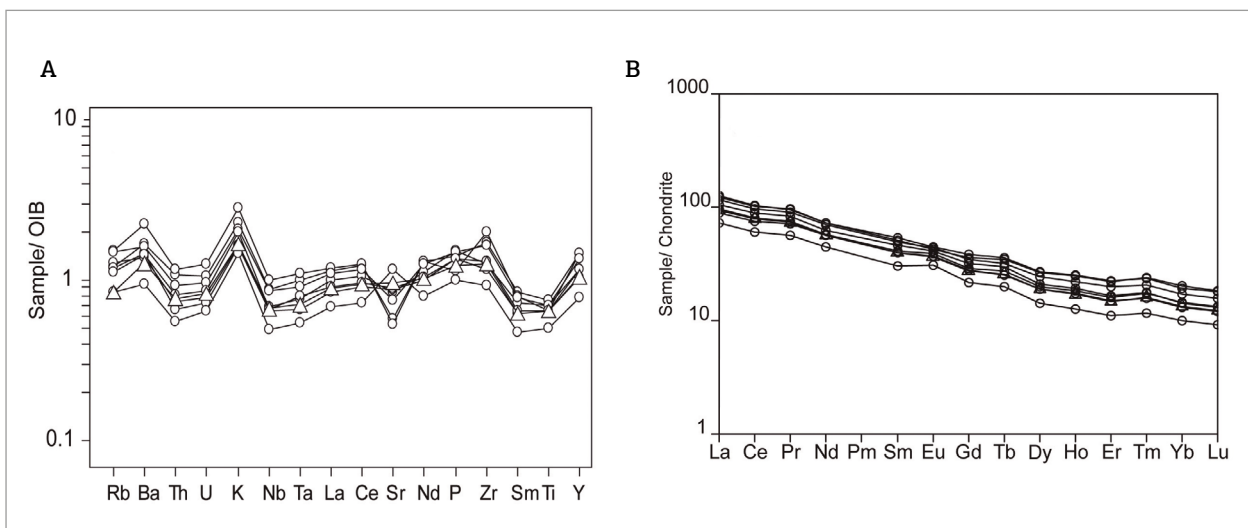


Figure 6. Multielementary diagram of the Cerro Morado rocks (cf. Alexandre *et al.* 2009). (A) Distribution of the trace elements normalized to OIB (Sun & McDonough 1989); (B) rare earth elements diagram normalized to chondrites (Nakamura 1974).

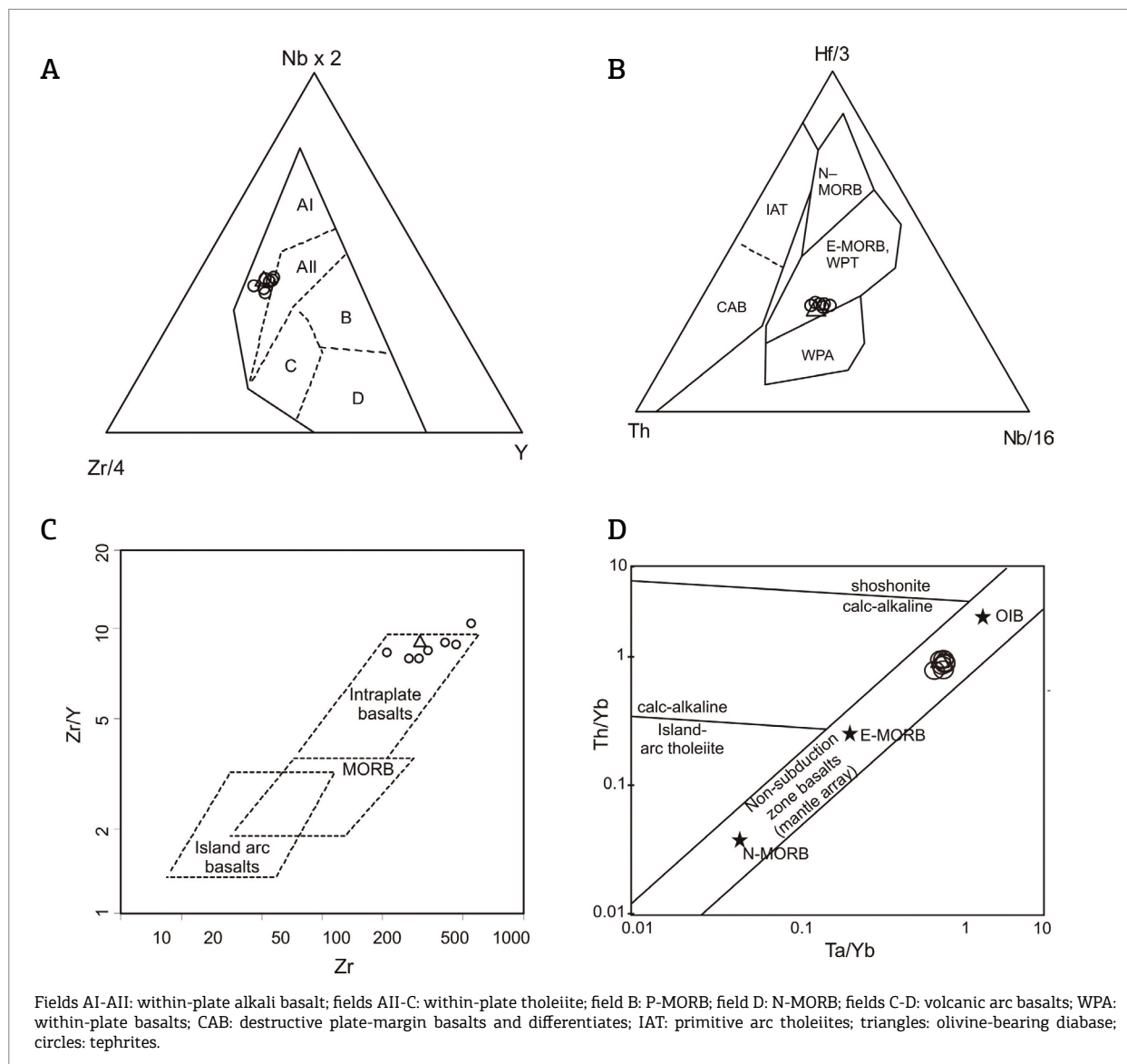


Figure 7. Cerro Morado samples plotted in diagrams of tectonic environment (cf. Alexandre et al. 2009). (A) Zr/4-Y-Nbx2 diagram (Meschede 1986); (B) Th-Hf/3-Nb diagram (Wood 1980); (C) Zr-Zr/Y diagram (Pearce & Cann 1973); (D) Th/Yb versus Ta/Yb diagram showing the samples plot between the OIB and E-MORB signatures (Pearce 1983).

Table 2. Isotopic compositions of Sr, Nd, and Pb of the Cerro Morado rocks in the Ischigualasto-Villa Union Basin.

Sample No.	Rock type	$(^{87}\text{Sr}/^{86}\text{Sr})$	2σ	$(^{87}\text{Sr}/^{86}\text{Sr})_t$	$(^{147}\text{Sm}/^{144}\text{Nd})$	$(^{143}\text{Nd}/^{144}\text{Nd})$	2σ	$(^{143}\text{Nd}/^{144}\text{Nd})_t$	$\epsilon_{\text{Nd}(0)}$	$\epsilon_{\text{Nd}(228)}$	$T_{\text{DM}}(\text{Ma})$	$(^{206}\text{Pb}/^{204}\text{Pb})$	ϵ	$(^{207}\text{Pb}/^{204}\text{Pb})$	2σ	$(^{206}\text{Pb}/^{204}\text{Pb})$	2σ
TM-04a	Tephrite	0.70437	0.003	0.70383	0.1361	0.512935	8	0.512731	5.8	7.6	254	18.347	0.0030	15.514	0.0019	37.872	0.0030
TM-06b	Tephrite	0.70381	0.002	0.70343	0.1340	0.513021	19	0.512821	7.5	9.3	93	18.327	0.0036	15.518	0.0023	37.853	0.0036
TM-07a	Tephrite	0.70461	0.002	0.70386	0.1344	0.512926	17	0.512725	5.6	7.4	264	18.357	0.0031	15.511	0.0019	37.879	0.0031
TM-08b	Tephrite	0.70366	0.002	0.70330	0.1347	0.513007	16	0.512806	7.2	9.0	119	18.319	0.0034	15.513	0.0022	37.834	0.0034
TM-09a	Tephrite	0.70385	0.003	0.70332	0.1348	0.512910	6	0.512708	5.3	7.1	295	18.351	0.0039	15.509	0.0025	37.867	0.0039
TM-10	Tephrite	0.70363	0.003	0.70331	0.1346	0.512933	7	0.512732	5.7	7.6	253	18.324	0.0070	15.515	0.0045	37.867	0.0070
TM-11	Tephrite	0.70345	0.002	0.70327	0.1324	0.513015	44	0.512818	7.4	9.2	102	18.321	0.0035	15.514	0.0022	37.840	0.0035
TM-12a	Olivine-bearing diabase	0.70336	0.002	0.70314	0.1330	0.512908	16	0.512709	5.3	7.1	293	18.353	0.0027	15.514	0.0017	37.881	0.0027

Initial ratios for Sr, Nd and epsilon values corrected to 228 Ma. Pb ratios are measured.

Sr-Nd-Pb isotope geochemistry of the Cerro Morado basic magmatism (NW Argentina): Implications for the mantle sources

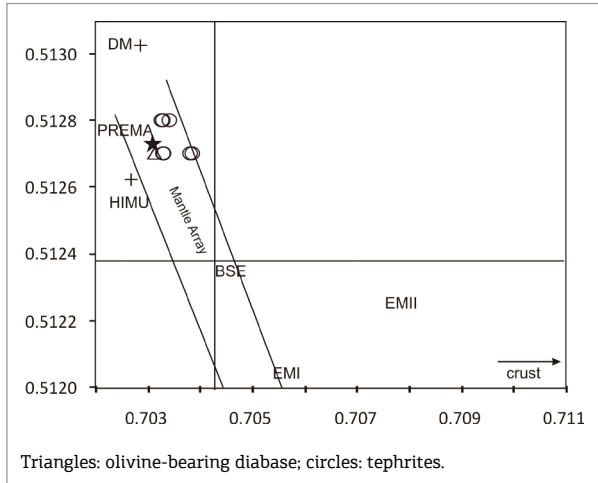


Figure 8. $^{143}\text{Nd}/^{144}\text{Nd}_i$ versus $^{87}\text{Sr}/^{86}\text{Sr}_i$ variation diagram for the studied hypabissais rocks. The mantle components DM, PREMA, HIMU, EM-I, and EM-II are taken from Zindler and Hart (1986). The mantle reservoir fields are those recalculated at 200 Ma by Deckart *et al.* (2005), close to the approximate crystallization age estimated for the Cerro Morado around 228 Ma. The mantle array position was recalculated at 285 Ma by Vozár *et al.* (2015), also close to the crystallization age of the Cerro Morado.

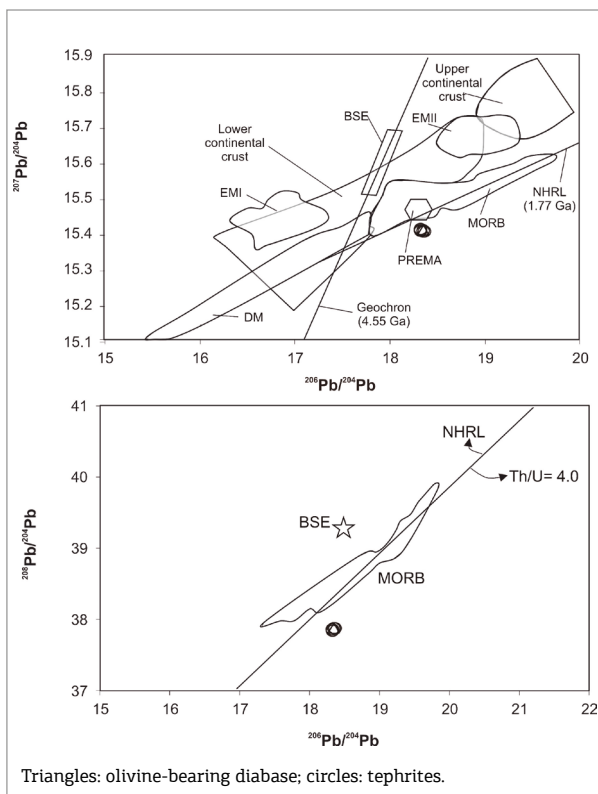


Figure 9. Lead isotope compositions for the studied rocks in comparison to mantle components PREMA, EM-I, EM-II, and DM (Zindler & Hart 1986). NHRL, Northern Hemisphere Reference Line (Hart 1984). The reservoirs fields are present-day Pb ratios.

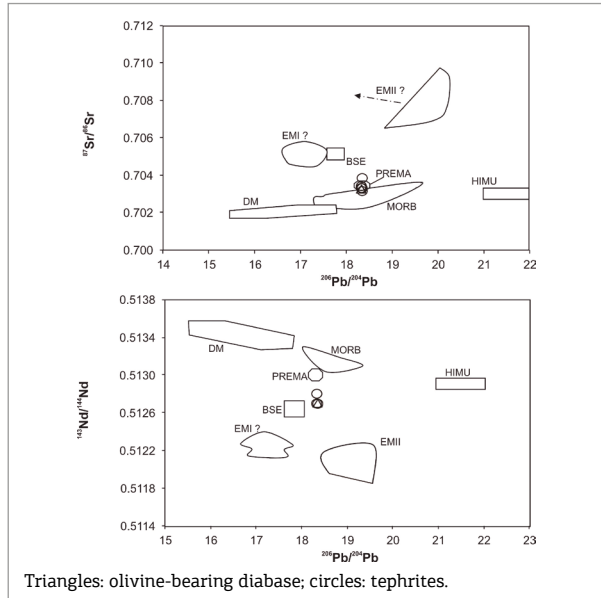


Figure 10. $^{87}\text{Sr}/^{86}\text{Sr}_i$ and $^{143}\text{Nd}/^{144}\text{Nd}_i$ against present-day Pb isotope compositions for the studied rocks compared to the fields of the mantle components HIMU, PREMA, EM-I, EM-II and DM (Zindler & Hart 1986).

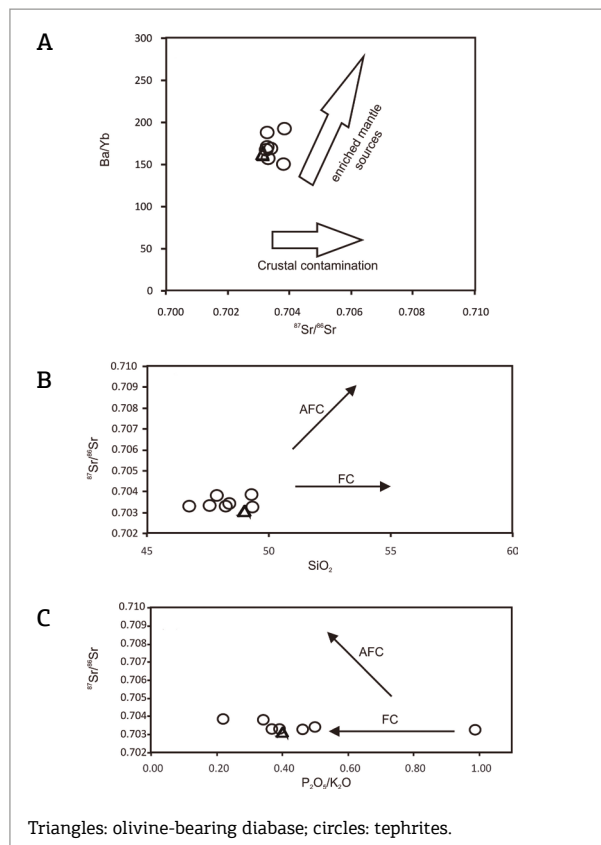


Figure 11. Diagrams indicative of crustal contamination. (A) Ba/Yb versus $^{87}\text{Sr}/^{86}\text{Sr}_i$ plot. The vectors are from Wilson (1989) and refer to open-system fractional crystallization (AFC) and closed-system fractional crystallization (FC); (B) plot of initial Sr isotope ratios versus SiO_2 (wt.%); (C) plot of initial Sr isotope ratios versus $\text{P}_2\text{O}_5/\text{K}_2\text{O}$.

(PREMA). The geochemical data suggest that this PREMA mantle source could have undergone modification due to interaction with crust in subduction modified by metasomatism. However, this alteration is restricted and was not identified by isotopes.

Additionally, the highly positive values of $\epsilon_{\text{Nd}(228 \text{ Ma})}$, Nd model ages younger than 295 Ma, low $^{87}\text{Sr}/^{86}\text{Sr}_i$ ratios and the lack of increasing $^{87}\text{Sr}/^{86}\text{Sr}_i$ value with increasing Ba/Yb ratios (Fig. 11A) and SiO_2 (Fig. 11B) suggest that there is no crustal contamination by rocks from the Precambrian basement during ascent of these magmas. Another sensitive indicator of crustal contamination is the $\text{P}_2\text{O}_5/\text{K}_2\text{O}$ ratio, since crustal rocks with silicic composition have $\text{P}_2\text{O}_5/\text{K}_2\text{O}$ generally lower than 0.1, while mantle derived magmas typically have high ratios (Carlson & Hart 1987, Hart *et al.* 1997). All the studied samples show values above 0.2, which reinforce the hypothesis that there is no significant crustal contamination (Fig. 11C).

In all diagrams involving Sr isotope ratios (Figs. 8, 9, 10 and 11), two samples (TM-04a, TM-07a) display slightly higher $^{87}\text{Sr}/^{86}\text{Sr}_i$ ratios (0.70383 and 0.70386), together with higher values of LOI (7.21 and 6.61%), Ba (635 and 859 ppm) and K_2O (2.63 and 3.28%), respectively, suggesting that these two samples may have undergone a slight crustal contamination, although the Nd isotopes have not been affected.

ACKNOWLEDGEMENTS

We acknowledge the financial support of the CNPq (projects: 303015/2015-2; 400724/2014-6, 441766/2014-5, 302213/2012-0, 303584/2009-2, 471402/2012-5, and 470505/2010-9). Acknowledgment is made to Editor Umberto Cordani and anonymous reviewers for valuable input and constructive reviews of this manuscript.

REFERENCES

- Alexandre F.P., Sommer C.A., Lima E.F., Chemale Jr. F., Marsicano C.A., Mancuso A.C., Brod J.A. (2009). Petrologia do magmatismo básico do Cerro Morado na bacia triássica Ischigualasto-Villa Unión (NW da Argentina). *Pesquisas em Geociências*, **36**:295-313.
- Bossi G.E. (1971). Análisis de la Cuenca de Ischigualasto - Ischichuá. In: Congreso Hispano-Luso-Americano de Geología Económica, 2, 611-626. Madrid-Lisboa: Ibérica-Tarragona.
- Carlson R.W., Hart W.K. (1987). Crustal genesis on the Oregon Plateau. *Journal of Geophysical Research*, **92**:6191-6206.
- Caselli A.T. (2000). Estudio sedimentológico de las formaciones Talampaya y Tarjados (Triásico Inferior) en el flanco occidental de la Sierra de Sanogasta, provincia de La Rioja (Argentina). In: 6 Reunión Sobre el Triásico Del Cono Sur, San Luis.
- Chemale Jr. F. Performed Ar-Ar dating in whole-rock and obtained ages of 228 ± 2 Ma. *Personal communication*, April 20, 2009.
- Cullers R.L., Graf J.L. (1984). Rare Earth Elements in Igneous Rocks of the Continental Crust: Intermediate and Silicic Rocks - Ore Petrogenesis. In: Henderson P. (ed.), *Rare Earth Element Geochemistry*, Amsterdam, Elsevier Science, p. 275-316.
- Deckart K., Bertrand H., Liégeois J.P. (2005). Geochemistry and Sr, Nd, Pb isotopic composition of the Central Atlantic Magmatic Province (CAMP) in Guyana and Guinea. *Lithos*, **82**:289-314.
- De Paolo D.J. (1981). Nd isotopic studies: Some new perspectives on Earth Structure and Evolution. *Earth and Space Science News*, **62**:137-145.
- Hart S.R. (1984). A large-scale isotope anomaly in the southern hemisphere mantle. *Nature*, **309**:753-757.
- Hart W.K., Carlson R.W., Shirey S.B. (1997). Radiogenic Os in primitive basalts from the northwestern U.S.A.: implications for petrogenesis. *Earth and Planetary Science Letters*, **150**:103-116.
- Kokogian D.A., Fernandes Seveso F., Lagarreta L. (1987). *Cuenca de Ischigualasto - Villa Unión: Análisis estratigráfico y caracterización paleoambiental*. Buenos Aires. (in press).
- Limarino C.O., Fauqué L., Caminos R. (1990). Fácies y evolución paleoambiental de los bancos rojos triásicos Del norte de la Precordillera riojana. In: Reunión Argentina De Sedimentología, San Juan, v. 1, 169-174.
- Lopez Gamundí O., Alvarez L., Andreis R., Bossi G.E., Espejo I., Fernández Seveso F., Legarreta I., Kokogian D.A., Limarino C.O., Sessarego H.L. (1989). Cuencas intermontanas. In: Chebli G.A., Spalletti L.A. (eds.), *Cuencas Sedimentarias Argentinas*. Tucumán, Universidad Nacional de Tucumán. Serie Correlación Geológica, v. 6, p. 123-167.
- Lugmair G.W., Marti K. (1978). Lunar initial $^{145}\text{Nd}/^{144}\text{Nd}$: differential evolution of the lunar crust and mantle. *Earth and Planetary Science Letters*, **39**:349-357.
- Meschede M. (1986). A method of discrimination between different types of mid-ocean ridge basalts and continental tholeiites with the Nb-Zr-Y diagram. *Chemical Geology*, **56**:207-218.
- Milana J.P., Alcober O.A. (1994). Modelo tectosedimentario de la cuenca triásica de Ischigualasto (San Juan, Argentina). *Revista de la Asociación Geológica Argentina*, **49**:217-235.
- Nakamura N. (1974). Determination of REE, Ba, Fe, Mg, Na and K in carbonaceous and ordinary chondrites. *Geochimica et Cosmochimica Acta*, **38**:757-775.
- Pearce J.A. (1983). Role of the sub-continental lithosphere in magma genesis at active continental margins. In: Hawkesworth C.J., Norry M.J. (eds.), *Continental Basalts and Mantle Xenoliths*. Nantwich, Shiva Publications, p. 230-249.
- Pearce J.A., Cann J.R. (1973). Tectonic setting of basic volcanic rocks determined by using trace element analyses. *Earth and Planetary Science Letters*, **19**:290-300.

Sr-Nd-Pb isotope geochemistry of the Cerro Morado basic magmatism (NW Argentina): Implications for the mantle sources

- Steiger R.H., Jäger E. (1977). Subcommittee on geochronology: Convention on the use of decay constants in geo- and cosmochronology. *Earth and Planetary Science Letters*, **36**:359-362.
- Stipanovic P.N., Bonaparte, J.F. (1979). Cuenca Triásica de Ischigualasto - Villa Union (Provincias de La Rioja y San Ruan). In: Simpósio de Geologia Regional da Argentina, Córdoba, v. 1, 523-575.
- Sun S.S., McDonough W.F. (1989). Chemical and isotopic systematics of oceanic basalts: implications for mantle composition and processes. In: Saunders A.D., Norry M.J. (eds.), *Magmatism in ocean basins*, London, Geological Society of London Special Publication, v. 42, p. 313-345.
- Thornton C.P., Tuttle O.F. (1960). Chemistry of igneous rocks. Differentiation index. *American Journal of Science*, **258**:664-684.
- Vozár J., Spisiak J., Vozárová A., Bazarnik J., Král J. (2015). Geochemistry and Sr, Nd isotopic composition of the Hronic Upper Paleozoic basic rocks (Western Carpathians, Slovakia). *Geologica Carpathica*, **66**:3-17.
- Wilson M. (1989). *Igneous Petrogenesis: a global tectonic approach*. London, Springer.
- Winchester J.A., Floyd P.A. (1977). Geochemical discrimination of different magma series and their differentiation products using immobile elements. *Chemical Geology*, **20**:325-343.
- Wood D.A. (1980). The application of a Th-Hf-Ta diagram to problems of tectonomagmatic classification and to establishing the nature of crustal contamination of basaltic lavas of the British Tertiary Volcanic Province. *Earth and Planetary Science Letters*, **50**:11-30.
- Zindler A., Hart S. (1986). Chemical geodynamics. *Annual Review of Earth and Planetary Sciences*, **14**:493-571.

